Design and Performance of Coplanar Waveguide Bandpass Filters

DYLAN F. WILLIAMS AND S. E. SCHWARZ, SENIOR MEMBER, IEEE

Abstract—**End-coupled resonator bandpass filters built in coplanar waveguide are investigated. The admittance inverter parameters of the coupling gaps between resonant sections are deduced from experiment, and bandpass filter design rules are developed. This allows easy filter synthesis from "prototype" low-pass designs. Measurements of single section resonator quality factors are used to predict filter insertion losses. Several examples of filters realized in coplanar waveguide are presented. Odd-mode coplanar waveguide filter elements that shortcircuit the even coplanar waveguide mode are investigated. Filter tuning, accomplished by adjusting the height of conducting planes above the resonant filter sections, is demonstrated.**

I. INTRODUCTION

DEVICES FOR operation at millimeter wavelengths have small dimensions. It is convenient to fabricate such devices using photolithography, but this requires that they be planar, or as nearly so as possible. Four guides that are easily produced photolithographically are microstrip, slotline, coplanar strips, and coplanar waveguide (CPW) [1], as shown in Fig. 1. These guides are open structures, and do not require precisely machined metallic enclosures.

Recently there has been considerable interest in using coplanar waveguide in millimeter-wave integrated circuits [2]–[4]. CPW is planar, permits both series and shunt connection of circuit elements, and has low radiation losses in the odd mode (opposing electric fields). CPW parameters are not sensitive functions of substrate thickness, and a wide range of impedance is achievable on reasonably thick substrates. Also, circuits can be built using both the odd and the even (electric fields in the same direction) CPW modes. Microstrip, the usual choice for integrated circuits, possesses some of the desirable properties of CPW. It has the advantage of familiarity; many well-characterized microstrip circuits are available. Microstrip, however, is not a truly planar guide, as the ground plane is on the bottom surface of the dielectric. While it is usually not difficult to construct the required ground plane, shunt connection of circuit elements is quite awkward, especially in the millimeter-wave region. Moreover, microstrip impedance and guide wavelength are undesirably sensitive functions of substrate thickness.

Manuscript received October 19, 1982; revised February 15, 1983. This work was supported in part by the U. S. Army Research Office under Contract DAAG29-82-K-0166, in part by the National Science Foundation under Grant ECS-8116018, in part by the Joint Services Electronics Program under AFOSR Grant F49620-79-C-0178, and in part by the U. S. Army MERADCOM under Grant DAAK 70-80-C-0134.

The authors are with the Department of Electrical Engineering and Computer Sciences and the Electronics Research Laboratory, University of California, Berkeley, CA 94720.

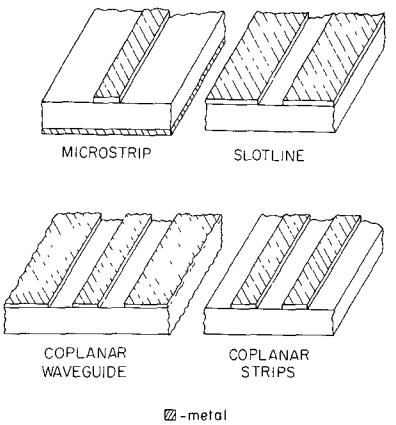

Fig. 1. Four open guiding structures.

In contrast to microstrip, there are fewer well-known CPW circuits, although the guide itself has been well characterized [1]–[10]. There has been considerable work on CPW directional couplers [1], [2], [7]–[9], and on mixer circuits using CPW [1]–[4], [11]–[20], and some on nonreciprocal CPW devices [21], planar antennas with CPW feed lines [22], and a magic T in CPW [23]; but with the exception of the papers by Houdart [2] and Holder [24], which present some mixer, filter, and diplexer circuits utilizing CPW and slotline, there has been no work, to the authors' knowledge, on filters using CPW. Previously, end-coupled resonator bandpass filters have been realized in many guiding structures including conventional waveguide and coaxial lines [25]–[27], microstrip [25], stripline [25], [27], and finline [28]–[30]. In this paper, we shall discuss the design and performance of end-coupled resonator bandpass filters realized in CPW. As will be seen, CPW is a guide well suited for this type of filter.

End-coupled resonant CPW filters are realized by cutting gaps in the inner conductor of the guide, thus creating capacitively coupled resonant sections as shown in Fig. 2. This filter structure retains all of the advantages of CPW including complete planarity, low radiation losses, and insensitivity to substrate thickness, and is well suited to monolithic millimeter-wave integrated circuitry. Filter design is accomplished by a synthesis technique [25]–[27] applicable to bandpass filters with fractional bandwidth less than 20 percent, utilizing the concept of admittance inverters (ideal quarter-wavelength transformers). This procedure is reviewed in Section II. Realization of the desired admittance inverters using gaps in the center conductor of CPW is discussed in Section III. To facilitate determina-

0018-9480/83/0700-0558$01.00 ©1983 IEEE

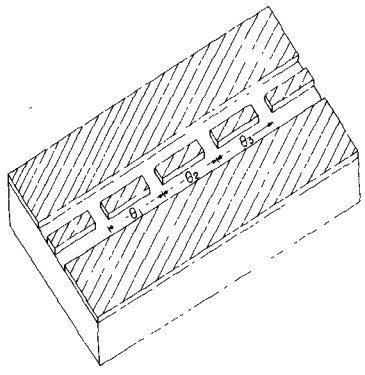

Fig. 2. Three-section bandpass filter in CPW.

tion of gap geometry and spacing, design information is presented in graphical form. A filter coupling element that presents a short circuit to the even mode propagating in the CPW is also described. Measurements of the unloaded quality factors of single resonant sections of CPW are used to predict filter insertion losses. In Section IV, the performance of several CPW bandpass filters is described. Filter tuning, accomplished by the use of conducting planes suspended at adjustable heights above the guide, is also demonstrated in this section. Performance at near-millimeter wavelengths is considered in Section V.

II. Design Principles

The bandpass CPW filters demonstrated in this work are designed using filter synthesis techniques for gap-coupled resonators as outlined by Matthaei, Young, and Jones [25] and Collins [26], and developed by Cohn [27]. We begin with a "prototype" low-pass filter as shown in Fig. 3(a), with element values g_i and the response shown in Fig. 3(b). The quantity g_i is the inductance of a series coil or the capacitance of a shunt capacitor for $i=1$ to n. The quantities g_0 and g_{n+1} are the generator and load impedances, respectively, when g_1 corresponds to a capacitor and the designs are symmetrical, as they are here. The g_i are normalized to make $g_0=1\ \Omega$ and $\omega_1'=1$ rad/s, where ω_1' is the prototype filter cutoff frequency, as shown in Fig. 3(b). The element values g_i are defined for more general circuit configurations and are conveniently tabulated for many desired responses in [25]. Here they were chosen to give a 0.2-dB Chebyshev response. The "prototype" low-pass filter of Fig. 3(a) is transformed to the lumped element bandpass filter of Fig. 3(c) with response shown in Fig. 3(d). The passbands are transformed according to

$$\omega' = \frac{\omega_1'}{w}\left(\frac{\omega}{\omega_0} - \frac{\omega_0}{\omega}\right) \tag{1}$$

$$w = \frac{\omega_2 - \omega_1}{\omega_0} \tag{2}$$

$$\omega_0 = \sqrt{\omega_1 \omega_2} \tag{3}$$

where ω and ω' are the angular frequencies in the bandpass and low-pass domains, respectively, and ω_0, ω_1, and ω_2 are the center, lower cutoff, and upper cutoff angular frequencies in the bandpass domain, as shown in Fig. 3(d). The

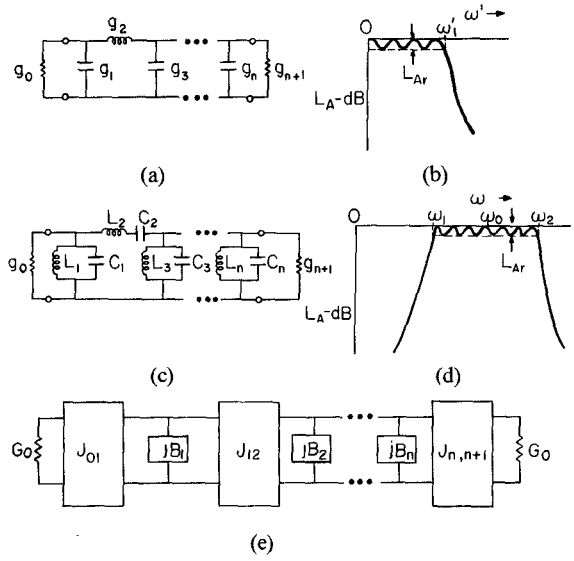

Fig. 3. Prototype low-pass, lumped element bandpass, and admittance inverter bandpass filters. (a) The prototype low-pass circuit and (b) its frequency response. (c) The lumped-element bandpass circuit and (d) its frequency response. (e) A schematic of a bandpass filter using admittance inverters. L_A and L_{Ar} are the filter attenuation and passband ripple, respectively.

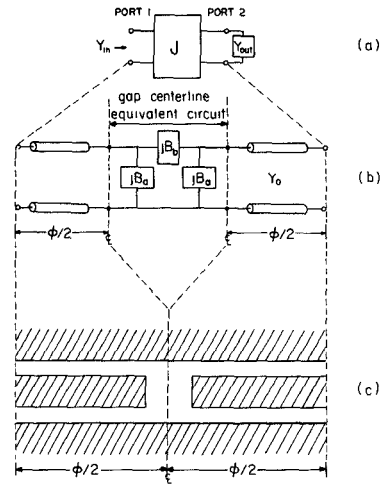

Fig. 4. Admittance inverters. (a) An ideal schematic representation. (b) A circuit representation. (c) The realization in CPW.

quantity w, defined by (2), is the fractional bandwidth of the bandpass filter.

The lumped-element circuit of Fig. 3(c) can be transformed to the circuit of Fig. 3(e), which has the same frequency response and is in a form that can be easily realized in CPW. All of the susceptances $B_j(\omega)$ were chosen to be identical in this work. This results in a considerable simplification, allowing the $B_j(\omega)$ to be realized as sections of CPW which are one-half wavelength long at the filter center frequency and of characteristic admittance Y_0, the characteristic admittance of the system. The boxes marked $J_{j,j+1}$ are admittance inverters. An admittance inverter is an ideal quarter-wavelength transformer. The admittance Y_{in} seen at port one is related to the admittance Y_{out} at port two (see Fig. 4(a)) by

$$Y_{in} = J^2 / Y_{out}. \tag{4}$$

With the choice of the $B_j(\omega)$ described above, the admittance inversion parameters J/Y_0 required to produce the response of Fig. 3(d) are given by [25]

$$J_{01}/Y_0 = J_{n,n+1}/Y_0 = \sqrt{\pi w/(2g_0 g_1 \omega_1')} \quad (5)$$

$$J_{j,j+1}/Y_0 = \pi w/\left(2\omega_1'\sqrt{g_j g_{j+1}}\right), \qquad j \neq 0, n \quad (6)$$

for symmetrical designs, where n is the number of resonant sections. The J's, like the g's in the low-pass domain, now determine the filter response in the bandpass domain. The admittance inverters are realized as adjustable gaps between the half-wavelength sections of CPW, as described in the following section.

III. Realization of Admittance Inverters in CPW

A. Circuit Description

The ideal admittance inverters just introduced can be approximated by the equivalent circuit of Fig. 4(b). The electrical line length ϕ is chosen to be [25]

$$\phi = -\tan^{-1}(2B_b/Y_0 + B_a/Y_0) - \tan^{-1}(B_a/Y_0). \quad (7)$$

The admittance parameter J is then given by

$$J/Y_0 = |\tan(\phi/2 + \tan^{-1}(B_a/Y_0))|. \quad (8)$$

The portion of Fig. 4(b) labeled "gap centerline equivalent circuit" is realized as the centerline equivalent circuit of the gap shown in Fig. 4(c). The centerline equivalent circuit of the gap is defined by its S-parameters with the reference planes of port 1 and port 2 lying in coincidence at the centerline position, marked $\mathcal{L}$ in Fig. 4(c). Two sections of CPW waveguide complete the circuit. The electrical length of these CPW sections computed from (7) is negative for most gap configurations. The negative electrical lengths are realized by combining these sections with the half-wavelength resonators, as shown in Fig. 5. The electrical length of the jth section is given by

$$\theta_j = \pi + (\phi_{j-1,j} + \phi_{j,j+1})/2 \quad (9)$$

where $\phi_{j,j+1}$ is computed from (7) for the gap that separates resonator j from resonator $j+1$.

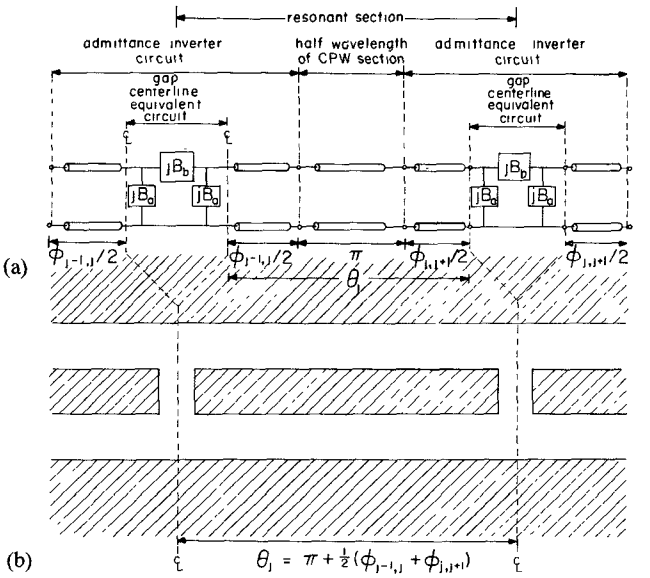

Fig. 5. A resonant section of CPW with gaps. (a) The circuit representation and (b) its realization in CPW.

TABLE I
Dimensions for Fig. 6, Normalized to the Free-Space Wavelength

1	$10^3 x_1/\lambda_0$
1	4.13
2	41.28
3	10.32
4	22.70
5*	6.19
6*	4.13
7	16.51
8	30.96
9	66.04
10	49.53

Note: The "bulge" in Fig. 6(b) associated with x_5 and x_6 results from the technique of fabrication and probably contributes no useful effect.

B. Physical Configurations

The physical configurations of the gaps are sketched in Fig. 6. Actual dimensions are listed in Table I. Large values of J were achieved through the use of interleaved fingers (Fig. 6(a) and (b)), as suggested by Houdart [2], while small values of J were obtained with simple gaps (Fig. 6(c)). As will be seen, the interleaved fingers give lower radiation loss for the same value of J.

The inverters shown in Fig. 6 were built in 50-Ω CPW with internal conductor width (x_4) of $22.7 \times 10^{-3}\lambda_0$, where λ_0 is the free-space wavelength. The spacing between the center conductor and the outer conductor was $13.41 \times 10^{-3}\lambda_0$ in all cases. The substrate's low-frequency dielectric constant was found from low-frequency capacitance measurements to be approximately 11.4, close to those of the silicon or GaAs substrates that might be used for monolithic integrated circuits in the millimeter-wave region. At millimeter wavelengths, thick substrates, which are easier to process, are desirable. The maximum allowable substrate thickness is that at which the lowest order TE surface-wave mode begins to propagate. This maximum thickness was calculated to be $0.077\lambda_0$ for the dielectrics used in this work [3]. The first evanescent surface mode was experimentally observed at a thickness of $0.066\lambda_0$. The substrate thickness chosen for these experiments was $0.054\lambda_0$.

Another type of admittance inverter structure is shown in Fig. 6(d) and (e). These structures, which we shall call "overlaid gaps," have a metallic bridge connecting the two outer conductors of the CPW. The bridge is insulated from the center conductor by a dielectric layer. The purpose of these overlaid gaps is to short-circuit the even CPW mode.

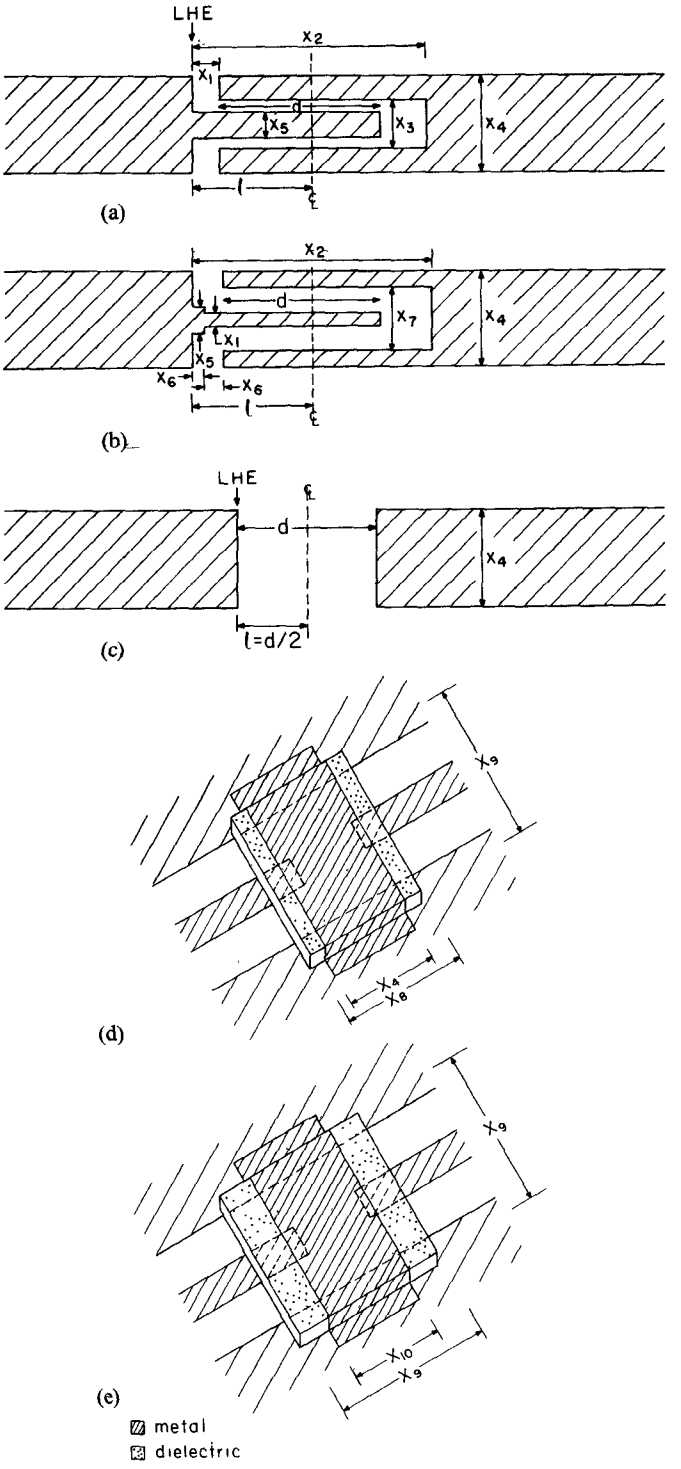

Fig. 6. Physical configurations of the admittance inverters. Only the center conductor is shown. Table I gives the normalized values of the x_i. The distance d is varied to give different values of the admittance inverter parameters J, ϕ, and l. The quantity l is the distance of the centerline equivalent circuit reference plane from the edge of the gap and is found from Fig. 9. Junction type b^* is the same as type b except that $x_2 = 24.76 \times 10^{-3} \lambda_0$. (d) and (e) depict overlaid gaps. The overlay dielectric is of thickness $3.1 \times 10^{-3} \lambda_0$, and has a dielectric constant of 7.3.

A dielectric of thickness $0.0031\lambda_0$, and dielectric constant 7.3 is placed over the active sections of the inverter gaps. The metal bridge is then placed over the dielectric and connected at its ends to the two ground planes. The distances separating the left-hand edges of the gaps of Fig. 6(a) and Fig. 6(c) (marked LHE in the figures) from the centers of the overlay structures are $x_1 + d/2$ and $d/2$, respectively. The even CPW mode is short-circuited, while the normal odd CPW mode is transmitted with high efficiency, so long as its frequency is within the filter passband. We note that although a single overlaid gap would suffice to reject the even mode, there would also be large reflections of the odd mode. In a filter, reflections of the odd mode can be made to cancel over the filter passband, so that nearly perfect transmission is obtained.

C. S-Parameter Measurements

Measurements of the junction's S-parameters were made as functions of d. From these we calculate the equivalent circuit elements B_b and B_a. The imaginary parts of B_b and B_a are small and, for now, are neglected. We then calculate J and ϕ from (7) and (8). The condition $\angle S_{11} = \angle S_{22}$ was used to determine l, the distance between the left-hand edge of the gap and the reference plane defining the gap's electrical centerline, as shown in Fig. 6. Plots of J/Y_0, ϕ, and l/λ_0 versus the normalized length d/λ_0 are given by the solid curves in Figs. 7, 8, and 9, respectively. (The data points indicated by circles, squares, and triangles will be considered later.) These curves can be used for filter design as follows. After calculating the values of J/Y_0 from the procedure in Section II, suitable gap types and their corresponding values of d/λ_0 are found from Fig. 7. Values of ϕ for each gap are then found from Fig. 8 and the physical distance between gap centerlines calculated from (9). Physical gap positions with respect to the centerline positions are determined from Fig. 9.

D. Excess Filter Loss

The excess filter loss L is defined as the extra loss at the center frequency, due to radiation, metallic, and dielectric losses, in a real filter that is not present in the ideal filter built with lossless elements. The data of Figs. 7, 8, and 9 do not allow prediction of the excess filter loss. In fact, the imaginary parts of B_b and B_a were neglected in the calculations leading to Figs. 7, 8, and 9. In any case, the S-parameter measurements are not sufficiently precise for accurate determination of the imaginary parts of B_b and B_a or the excess filter loss. The excess loss at the filter center frequency can be estimated, however, by the formulas due to Cohn [31], [25]

$$L = 4.343 \sum_{k=1}^{n} d_k g_k \,(\mathrm{dB}) \tag{10}$$

and

$$d_k = \omega_1' / (w Q_{u,k}) \tag{11}$$

where $Q_{u,k}$ is the unloaded quality factor of the kth resonant section, and n, g, w, and ω_1' are as defined earlier. The unloaded quality factor Q_u is the quality factor of the resonant section of Fig. 5, with all energy dissipation in the circuit due to radiation, ohmic, or dielectric losses, and with no external loading. To obtain accurate values of Q_u, we have performed transmission measurements on single resonant sections like those of Fig. 5, with several kinds of

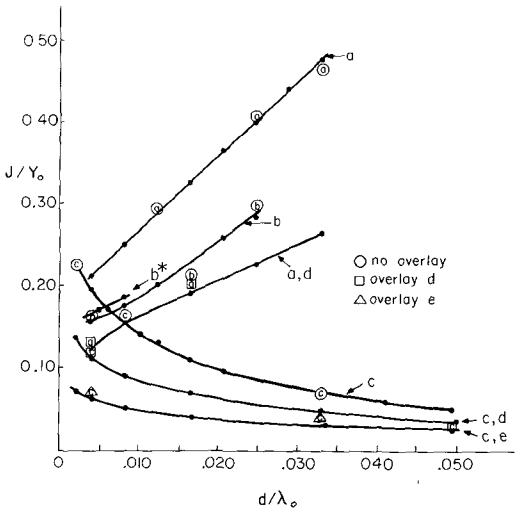

Fig. 7. J/Y_0 as a function of d/λ_0. Letters on solid curves refer to the gap types of Fig. 6. (For example, "a" means gap of Fig. 6(a) with no overlay; "a, d" means gap of Fig. 6(a) with the overlay of Fig. 6(d).) The solid curves represent data derived from S-parameter measurements. Letters inside circles, squares, and triangles refer to gaps with no overlay, to the overlaid gaps of Fig. 6(d), and to the overlaid gaps of Fig. 6(e), respectively, and represent data derived from resonant section measurements.

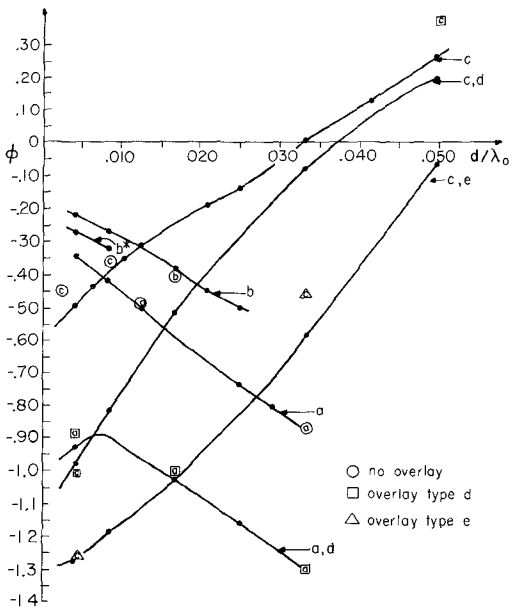

Fig. 8. The quantity ϕ (see (7) in the text) as a function of d/λ_0. The key to the symbols is the same as for Fig. 7.

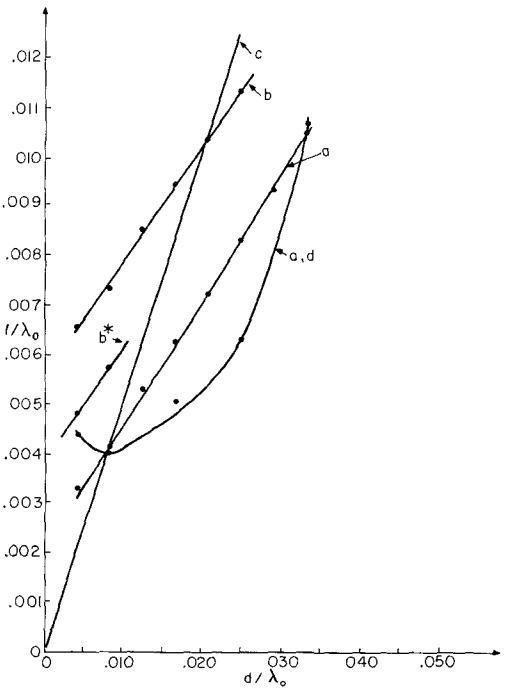

Fig. 9. The quantity l/λ_0, the distance to the gap's electrical centerline, is plotted as a function of d/λ_0. The key to the symbols is the same as for Fig. 7.

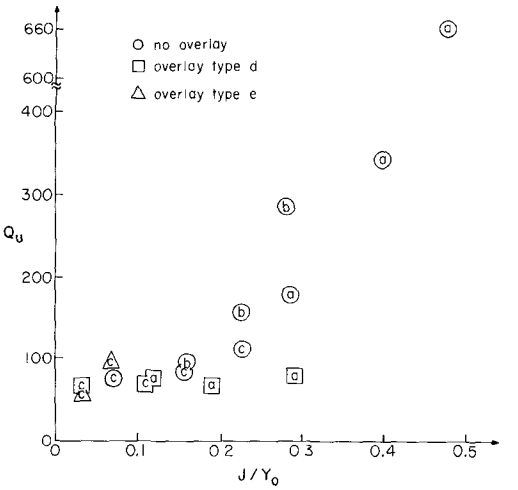

Fig. 10. Measured values of single resonant section unloaded quality factors are plotted as a function of J/Y_0. Letters refer to the gap types of Fig. 6. Letters inside circles, squares, and triangles refer to gaps with no overlay, to the overlaid gaps of Fig. 6(d),and to the overlaid gaps of Fig. 6(e), respectively.

terminating gaps. This was done by determining the center frequency f_s, the 3-dB bandwidth $f_{3\text{dB}}$, and the center frequency excess loss L_s of a single resonant section and using the relations [25]

$$Q_L = f_s/f_{3\text{ dB}} \tag{12}$$

$$Q_e^2 = 4Q_L^2 10^{L_s/10L_s} \tag{13}$$

$$Q_u^{-1} = Q_L^{-1} - 2Q_e^{-1} \tag{14}$$

where L_s is in decibels. The external quality factor Q_e is the quality factor that the resonant section would have if there were no radiation, ohmic, or dielectric losses, all damping in that case being due to the external circuit. The loaded quality factor Q_L is the quality factor of the resonant section including radiation, ohmic, and dielectric losses, as well as the external loading of the measurement apparatus.

Fig. 10 shows the resulting values of Q_u for different gap configurations as a function of J/Y_0. The measurements were performed at $f_0 = 0.78$ GHz, where the measured Q_u were dominated by radiation losses. To obtain minimum-loss filters, the gap type with the highest Q_u for a desired J/Y_0 should be chosen. Reference to Fig. 10 shows that the type b gap is preferable to either type a or c gaps for comparable values of J/Y_0. This can be explained qualitatively in the following way. Type c gaps have the largest radiation loss because the electric fields in the gaps radiate

as two simple dipoles, one at each end of the resonant section. In the type *b* gap, the electric fields are roughly in opposite directions and radiate as two quadrupoles, dissipating less energy. As J/Y_0 increases, the gap center conductor length d increases, and the fields become more nearly opposite in direction, lowering the radiation losses further. For values of J/Y_0 of approximately 0.3, the center conductor length d of the type *a* gap is still short, and fields are not completely opposite, resulting in higher radiation losses than the type *b* gap, which has a long center conductor length for $J/Y_0 = 0.3$. For larger values of J/Y_0 in type *a* gaps, d increases, the fields become more nearly opposite in direction, and radiation losses decrease.

The synthesis technique outlined in Section II will not give filters with precise equiripple characteristics or minimum achievable losses. This is because the finite resonant section unloaded quality factors were not considered in the synthesis procedure. Precise minimum-loss, equiripple, or maximally flat filters can be designed using the unloaded quality factors from Fig. 10 and the synthesis techniques presented by Taub and Bogner [32], Fubini and Guillemin [33], and Dishal [34]. Cohn [31] presents a useful comparison of these synthesis techniques.

E. Comparision of Measurements

We are now in position to verify the gap admittance parameters J and ϕ using the single-resonant-section transmission measurements. J is calculated from [25]

$$J/Y_0 = \sqrt{\pi/2Q_e} \tag{15}$$

and ϕ is calculated from

$$\phi = \phi_s + \pi(f_s - f_0)/f_0 \tag{16}$$

where f_0 is the design center frequency and ϕ_s is the value of ϕ used in the design of the resonant section. The quantity ϕ_s was found from Fig. 8 and was derived from the S-parameter measurements described above.

Figs. 7 and 8 show good agreement between J and ϕ calculated from S-parameters (solid lines) and J and ϕ calculated from resonant section measurements (circled letters) for gaps without overlays. Fig. 7 also shows the good agreement between J calculated from S-parameters and J calculated from resonant section measurements (letters in squares or triangles) for the overlaid gaps. Experimental difficulties with the overlaid gaps limited the accuracy of the phase measurements of S_{11} and S_{22}, reducing the accuracy of the overlaid gap data derived from S-parameter measurements shown in Figs. 8 and 9. The values of ϕ derived from resonant section measurements for overlaid gaps are believed to be more accurate than those values of ϕ derived from S-parameter measurements for the overlaid gaps in Fig. 8.

IV. CPW Bandpass Filter Examples

In order to verify the design data given in the previous sections, several 3-section 0.2-dB Chebyshev filters were built with different bandwidths. The filter design parameters are summarized in Table II. The filters were built with a center frequency of 0.78 GHz. Predicted excess losses were calculated using Fig. 10 and (10), and are presented in Table II. Unloaded quality factors for resonant sections with different gaps on either end were estimated to be

$$Q_u = 2/\left(Q_{u1}^{-1} + Q_{u2}^{-1}\right) \tag{17}$$

where Q_{u1} and Q_{u2} are the single-section resonant radiation quality factors associated with the two gaps.

TABLE II
Filter Design Parameter Summary

		1ST ADMITTANCE INVERTER			2ND ADMITTANCE INVERTER			L	
Fig.	w	Type	J_{01}/Y_0	Q_u	Type	J_{12}/Y_0	Q_u	Predicted	Measured
11[1]	.177	Fig. 6(a)	.476	660	Fig. 6(b)	.234	160	.41 dB	.45 dB
12[1]	.13	Fig. 6(a)	.408	350	Note 4	.172	110	.84 dB	.93 dB
13(a)[1]	.047	Fig. 6(a)	.245	190	Fig. 6(c)	.062	75	3.5 dB	5.5 dB
13(b)[2]	.047	Fig. 6(b)	.245	190	Note 5	.062	95	2.9 dB	6.0 dB
13(c)[3]	.047	Fig. 6(b)	.245	190	Fig. 6(c)	.062	75	3.5 dB	2.7 dB

For the 3-section 0.2-dB Chebyshev filters in this paper, $g_0 = g_4 = 1.0$, $g_1 = g_3 = 1.2275$, and $g_2 = 1.1525$.

Notes: [1]Untuned, no overlay. [2]Untuned, with overlay. [3]Tuned, no overlay. [4]Same as Fig. 6(b) but with $x_2 = 24.7 \times 10^{-3}\lambda_0$. [5]Gap of Fig. 6(c) with overlay of Fig. 6(e).

Figs. 11 and 12 show the measured and ideal transmission characteristics of filters with $w = 0.177$ and 0.13, respectively. The predicted and measured transmission characteristics are in good agreement. In the filter transmission characteristic of Fig. 11, even the 0.2-dB Chebyshev ripples are apparent. The minimum filter losses of 0.45 dB and 0.93 dB are quite low, and are close to the predicted excess losses of 0.41 dB and 0.84 dB shown in Table II. Equations (10) and (11) predict even lower excess loss for wider bandwidth filters. This is because the term wQ_u appears in the denominator of (11) and, as can be seen from (5), (6), and Fig. 10, is an increasing function of w.

Fig. 13 shows the response curves of three narrow-band filters with $w = 0.047$. The filter of Fig. 13(a) is built without using overlaid gaps. The filter of Fig. 13(b) was built with overlaid gaps, and short-circuits the even CPW mode. While the fractional bandwidths and out-of-band attenuation characteristics of the filters in Fig. 13(a) and (b) are roughly as predicted, the center frequencies and midband transmission losses are not. It is apparent from a comparison of Figs. 11, 12, and 13 that the moderate bandwidth filters of Figs. 11 and 12 perform adequately as designed with no further adjustments necessary, while the narrow bandwidth filters of Fig. 13(a) and (b) require tuning of the resonant sections to achieve the predicted performance.

Tuning of CPW resonant sections, as suggested by Wang and Schwarz [35], can be accomplished by placing metallic conducting planes above the CPW circuits. Fig. 13(c) shows the transmission loss for the filter of Fig. 13(a) when a conducting plane over the third resonant section was adjusted to a height of $0.026\lambda_0$ above the dielectric surface.

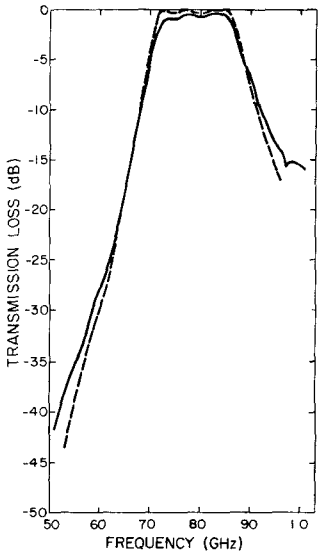

Fig. 11. Measured (solid line) and ideal (dashed lines) transmission curves for a 3-section CPW bandpass filter ($w = 0.177$).

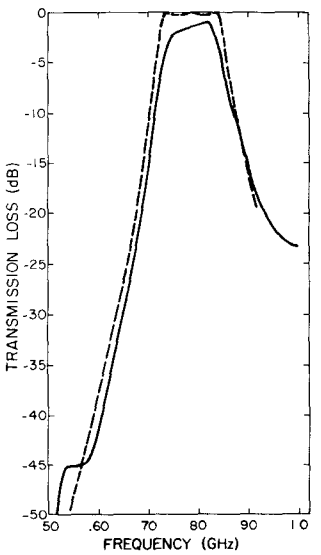

Fig. 12. Measured (solid line) and ideal (dashed lines) transmission curves for a 3-section CPW bandpass filter ($w = 0.13$).

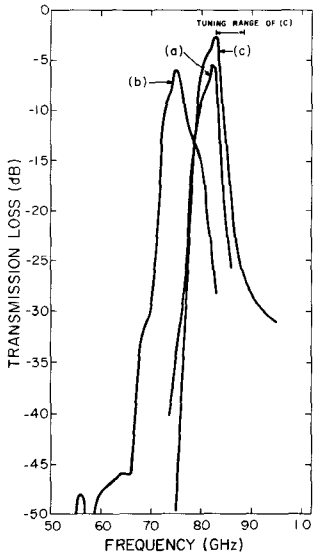

Fig. 13. Measured transmission curves for 3-section CPW bandpass filters ($w = 0.047$). (a) The response of an untuned filter with no overlay. (b) The response of an untuned filter with overlaid gaps. (c) The response of the filter of Fig. 13(a) after tuning.

The excess loss of the tuned filter of Fig. 13(c) was 2.7 dB, considerably less than the 5.5-dB excess loss of the similar, but untuned, filter of Fig. 13(a). The excess loss of the tuned filter of Fig. 13(c) was even lower than the 3.5-dB excess loss predicted in Table II. By placing adjustable conducting planes above all three resonant sections, the passband center frequency could be adjusted upward by 7 percent while maintaining the low filter loss and the passband shape of Fig. 13(c). Attempts to shift the center frequency further, however, resulted in distortion of the shape of the filter passband and increased excess loss.

V. Predicted Performance at Higher Frequencies

We envision the use of CPW filters in planar near-millimeter-wave technology. Thus, the question of ohmic losses at frequencies up to perhaps 100 GHz must be considered. Ohmic losses in CPW have been studied by a number of authors [1], [3], [4], [36]–[39]. Let us define an additional unloaded quality factor Q_{u0} for single resonant sections as the value that Q_u would take if ohmic losses, but not radiation losses, were present. Similarly, we define Q_{ur} as the unloaded quality factor including radiation losses, but not ohmic losses. Because the low frequency losses measured in the last section were dominated by radiation losses, for CPW we identify Q_{ur} with the Q_u plotted in Fig. 10. In estimating Q_{ur} we have assumed that the tolerances of photolithographic millimeter-wave structures will be at least as good as those of our microwave models. This assumption is valid for frequencies up to at least 150 GHz if a photolithographic resolution of one micron is used. The high-frequency unloaded Q, Q_{uh}, is then given by $Q_{uh}^{-1} = Q_{ur}^{-1} + Q_{u0}^{-1}$. Once the Q_{uh} are known, the excess filter loss can be obtained from (10).

Using data from Denlinger [36], we estimate Q_{u0} to be 350 at 75 GHz, although the actual value will depend on the smoothness of the metal surfaces and of the edges defined by the photolithographic process. Hence, at 75 GHz the filters of Figs. 11, 12, and 13 would have excess losses 0.25 dB, 0.34 dB, and 0.95 dB greater than those shown for 0.78 GHz, respectively. The excess filter losses would be 0.7 dB, 1.3 dB, and 3.7 dB, respectively. These losses are reasonably low for an open structure, and recommend CPW filters for use in the near-millimeter-wave region.

Bandpass filters at millimeter frequencies are most commonly realized in closed structures such as rectangular waveguide and coaxial line. Bandpass filters realized in finline [28], [29], a closed guiding structure, are particularly interesting as the filter elements are defined photolithographically. Losses of finline bandpass filters with fractional bandwidths less than 0.05 are at least 2 dB lower [28], [29] than those of comparable CPW filters in the

75-GHz range. (The transition loss necessary for integration of semiconductor devices with finline bandpass filters has been included.) At moderate fractional bandwidths (0.1–0.2), however, the losses of finline and CPW become comparable. From the results of Meier [30], we estimate the loss of a three-resonator finline bandpass filter with fractional bandwidth of 0.125, 75-GHz center frequency, and the appropriate transitions for semiconductor device integration to be 1.7 dB. This is to be compared with the 1.3-dB loss estimated above for a similar CPW bandpass filter. The great advantage of CPW over finline is, of course, its simplicity of manufacture and its compatibility with fully planar structures.

It is also interesting to compare the losses of CPW at near-millimeter wavelengths with those of microstrip, the most popular planar open guiding structure. Using data from Denlinger [36], Q_{u0} for microstrip is estimated to be 850 at 75 GHz. This is to be compared with the value of 350 for CPW. The microstrip resonant section has lower ohmic losses than the CPW resonant section because the fields in microstrip are not as concentrated at the conductor edges as they are in CPW. Radiation losses of gaps in microstrip, on the other hand, are somewhat larger, with the thick substrates desirable for millimeter-wave circuits. Assuming the same dielectric constant and substrate thickness, the value of Q_{ur} for a 50-Ω half-wavelength resonant section of microstrip is calculated by [36, eq. (15)] to be 22, if simple gaps such as those shown in Fig. 6(c) are assumed. This is to be compared with the value of 75 measured for a large simple-gap resonant section of CPW in this work. In order to obtain a comparison, we calculate the combined unloaded single-resonant-section quality factors Q_{uh} for resonant sections terminated in simple gaps. These are calculated to be approximately 62 for CPW sections and 21 for microstrip sections. Thus, at least for the case of simple gaps, the CPW filter is seen to have lower loss than its microstrip equivalent. This is due to the dominance of radiation losses in the case of simple gaps on thick substrates. With the gap types of Fig. 6(a) and (b), however, ohmic losses may be relatively more significant, and the advantage of CPW may become smaller or nonexistent.

VI. Conclusions

Our results show that high-efficiency bandpass filters can readily be built in planar form. Design is straightforward and leads to predictable results. Excess loss can also be estimated accurately in most cases. The minimum insertion loss of 0.45 dB measured at 0.78 GHz for a filter with a 17.7-percent fractional bandwidth is quite satisfactory for an open structure. Filters with fractional bandwidths smaller than 5 percent are also feasible, but require tuning. Special filters intended to block the even CPW mode have been demonstrated. Loss estimates indicate that CPW filters will continue to be useful at frequencies as high as 100 GHz.

The low radiation loss of CPW recommends it for use in planar integrated circuits. Integrated circuits with low-loss guides and tunable components may eventually become nearly as efficient as conventional waveguide systems.

Acknowledgment

The authors thank Nan-lei Wang for his assistance and encouragement.

References

[1] K. C. Gupta, R. Garg, and I. J. Bahl, *Microstrip Lines and Slotlines*. Dedham, MA: Artech House, 1979.

[2] M. Houdart, "Coplanar lines: Application to broadband microwave integrated circuits," in *Proc. Sixth Eur. Microwave Conf.*, 1976, pp. 49–53.

[3] R. A. Pucel, "Design considerations for monolithic microwave circuits," *IEEE Microwave Theory Tech.*, vol. MTT-29, pp. 513–534, June 1981.

[4] D. R. Ch'en and D. R. Decker, "MMIC's: The next generation of microwave components," *Microwave J.*, pp. 67–78, May 1980.

[5] T. Hatsuda, "Computation of coplanar-type strip-line characteristics by relaxation method and its application to microwave circuits," *IEEE Microwave Theory Tech.*, vol. MTT-23, pp. 795–802, Oct. 1975.

[6] T. Kitazawa and Y. Hayashi, "Coupled slots on an anistropic sapphire substrate," *IEEE Microwave Theory Tech.*, vol. MTT-29, pp. 1035–1040, Oct. 1981.

[7] J. B. Knorr and B. Kuchler, "Analysis of coupled slots and coplanar strips on dielectric substrate," *IEEE Microwave Theory Tech.*, vol. MTT-23, pp. 541–548, July 1975.

[8] C. P. Wen, "Coplanar-waveguide directional couplers," *IEEE Microwave Theory Tech.*, vol. MTT-18, pp. 318–332, June 1970.

[9] R. N. Simons, "Suspended broadside-coupled slot line with overlay," *IEEE Microwave Theory Tech.*, vol. MTT-30, pp. 76–81, Jan. 1982.

[10] T. Kitazawa and Y. Hayashi, "Quasi-static characteristics of coplanar waveguide on a sapphire substrate with its optical axis inclined," *IEEE Microwave Theory Tech.*, vol. MTT-30, pp. 920–922, June 1982.

[11] L. E. Dickens and D. W. Maki, "An integrated-circuit balanced mixer image and sum enhanced," *IEEE Microwave Theory Tech.*, vol. MTT-23, pp. 276–281, Mar. 1975.

[12] S. Dixon, R. J. Malik, J. Paul, P. Yen, T. R. Aucoin, and L. T. Yaun, "Subharmonic mixer using planar doped barrier diodes," in *Proc. IEEE MTT-S Int. Microwave Symp.*, 1982, pp. 27–29.

[13] L. Bui and D. Ball, "Broadband planar balanced mixers for millimeter-wave applications," in *Proc. IEEE MTT-S Int. Microwave Symp.*, 1982, pp. 204–205.

[14] L. Yuan, J. Paul, and P. Yen, "140 GHz quasi-optical planar mixers," in *Proc. IEEE MTT-S Int. Microwave Symp.*, 1982, pp. 374–375.

[15] J. K, Hunton and J. S. Takeuchi, "Recent developments in microwave slotline mixers and frequency multipliers," in *Proc. IEEE MTT-S Int. Microwave Symp.*, 1970, pp. 196–199.

[16] H. Ogawa, M. Akaike, M. Aikawa, T. Karaki, and J. Watanabe, "A 26-GHz band integrated circuit of a double-balanced mixer and circulators," *IEEE Microwave Theory Tech.*, vol. MTT-30, pp. 34–41, Jan. 1982.

[17] A. Cappello and J. Pierro, "A 22 to 24 GHz cryogenically cooled low noise FET amplifier in coplanar waveguide," in *Proc. IEEE MTT-S Int. Microwave Symp.*, 1982, pp. 19–22.

[18] J. K. Hunton, "A microwave integrated circuit balanced mixer with broad-bandwidth," in *Proc. IEEE MTT Microelectronics Symp.*, 1969, pp. A3.1–A3.2.

[19] B. J. Clifton, G. D. Alley, R. A. Murphy, and W. J. Piacentini, "Cooled low noise GaAs monolithic mixers at 110 GHz," in *Proc. IEEE MTT-S Int. Microwave Symp.*, 1981, pp. 444–446.

[20] J. Kohler and B. Schiek, "Broadband microwave frequency doublers," *Radio Electron. Eng.*, vol. 48, pp. 29–32, Jan./Feb. 1978.

[21] C. P. Wen, "Coplanar waveguide: A surface strip transmission line suitable for nonreciprocal gyromagnetic device applications," *IEEE Microwave Theory Tech.*, vol. MTT-17, pp. 1087–1090, Dec. 1969.

[22] A. Nesic, "Slotted antenna array excited by a coplanar waveguide," *Electron. Lett.*, vol. 18, no. 6, pp. 275–276, Mar. 1982.

[23] M. Aikawa and H. Ogawa, "A new MIC magic-T using coupled slotlines," *IEEE Microwave Theory Tech.*, vol. MTT-28, pp. 523–528, June 1980.

[24] P. A. R. Holder, "*X*-band microwave integrated circuits using slotline and coplanar waveguide," *Radio Electron. Eng.*, vol. 48, pp. 38–42, Jan./Feb. 1978.

[25] G. L. Matthaei, L. Young, and E. M. T. Jones, *Microwave Filters, Impedance-Matching Networks, and Coupling Structures.* New York: McGraw-Hill, 1964.
[26] R. E. Collin, *Foundations for Microwave Engineering.* New York: McGraw-Hill, 1966.
[27] S. B. Cohn, "Direct-coupled-resonator filters," *Proc. IRE*, vol. 45, pp. 187–196, Feb. 1957.
[28] F. Arndt, J. Bornemann, D. Grauerholz, and R. Vahldieck, "Theory and design of low-insertion loss fin-line filters," *IEEE Microwave Theory Tech.*, vol. MTT-30, pp. 155–163, Feb. 1982.
[29] A. M. K. Saad and K. Schunemann, "Design and performance of fin-line bandpass filters," in *Proc. Tenth European Microwave Conf.*, Sept. 1980, pp. 397–401.
[30] P. J. Meier, "Integrated fin-line millimeter components," *IEEE Microwave Theory Tech.*, vol. MTT-22, pp. 1209–1216, Dec. 1974.
[31] S. B. Cohn, "Dissipation loss in multiple-coupled-resonator filters," *Proc. IRE*, vol. 47, pp. 1342–1348, Aug. 1959.
[32] J. J. Taub and B. F. Bogner, "Design of three-resonator band-pass filters having minimum insertion loss," *Proc. IRE*, vol. 45, pp. 681–687, May 1957.
[33] E. G. Fubini and E. A. Guillemin, "Minimum insertion loss filters," *Proc. IRE*, vol. 47, pp. 37–41, Jan. 1959.
[34] M. Dishal, "Design of dissipative band-pass filters producing desired exact amplitude-frequency characteristics," *Proc. IRE*, vol. 37, pp. 1050–1069, Sept. 1949.
[35] N. Wang and S. E. Schwarz, "Planar oscillators for monolithic integration" *Int. J. Infr. Millimeter Waves*, vol. 3, pp. 771–782, Nov. 1982.
[36] E. J. Denlinger, "Losses of microstrip lines," *IEEE Microwave Theory Tech.*, vol. MTT-28, pp. 513–522, June 1980.
[37] A. Gopinath, "Losses in coplanar waveguides," *IEEE Trans. Microwave Theory Tech.*, vol. MTT-30, pp. 1101–1104, July 1982.
[38] B. E. Spielman, "Dissipation loss effects in isolated and coupled transmission lines," *IEEE Microwave Theory Tech.*, vol. MTT-25, pp. 648–655, Aug. 1977.
[39] J. A. Higgins, A. Gupta, G. Robinson, and D. R. Ch'en, "Microwave GaAs FET monolithic circuits," in *Int. Solid State Circuits Conf. Dig.*, 1979, pp. 20–21.

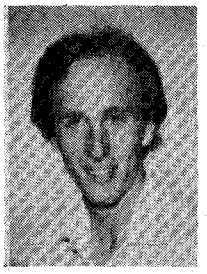

Dylan F. Williams was born in Boulder, CO, on December 19, 1955. He received B.A.'s in physics and mathematics from the University of Colorado in 1978.

He joined the Motorola Government Electronics Division and was engaged in research in surface acoustic-wave devices until 1981. He is currently a Research Assistant at the Department of Electrical Engineering and Computer Sciences, University of California, Berkeley.

Mr. Williams is a member of Phi Beta Kappa.

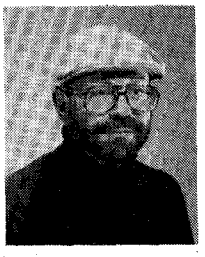

S. E. Schwarz (SM'71) was born in Los Angeles, CA, in 1939. He received the B.S. degree in physics from California Institute of Technology, Pasadena, in 1959, the A.M. from Harvard University, Cambridge, MA, in 1961, and the Ph.D. in electrical engineering from Cal Tech in 1964.

He has held positions with Hughes Research Laboratories, Bell Laboratories, and IBM Research Laboratories. Since 1964 he has been affiliated with the Department of Electrical Engineering and Computer Sciences at the University of California, Berkeley, where he is now a Professor, emphasizing millimeter-wave devices and integrated circuits.

Professor Schwarz held a Guggenheim Fellowship in 1971–72.